Author(s): Lei Chen, Shi-zhong Zheng, Zhi-guang Sun, Ai-yun Wang, Chen-hu Huang, Neville A. Punchard, Shi-le Huang, Xiang Gao, Yin Lu
Article Title: Cryptotanshinone has diverse effects on cell cycle events in melanoma cell lines with different metastatic capacity
Year of publication: 2011
Citation: Chen, L., Zheng, S.Z., Sun, Z.G., Wang, A.Y., Huang, C.H., Punchard, N.A., Huang, S.L., Gao, X., Lu, Y., 'Cryptotanshinone has diverse effects on cell cycle events in melanoma cell lines with different metastatic capacity' Cancer Chemotherapy And Pharmacology, 68(1), 17-27

Link to published version: doi:10.1007/s00280-010-1440-8

Cryptotanshinone has opposite effects on cell cycle events in melanoma cell lines with different metastatic capacity

Lei Chen [a], Shi-zhong Zheng [a], Zhi-guang Sun [a], Ai-yun Wang [a], Chen-hu Huang [a], Neville A. Punchard [c], Shi-le Huang [e], Xiang Gao [b,*], Yin Lu [a,d*]

[a] Department of Clinical Pharmacy, School of Pharmacy, Nanjing University of Chinese Medicine, Nanjing 210029, China;
[b] Model Animal Research Center, Nanjing University, Nanjing 210061, China;
[c] School of Health & Bioscience, University of East London, London, E15 4LZ, UK;
[d] Jiangsu Key Laboratory for Traditional Chinese Medicine Formulae Research, Nanjing University of Chinese Medicine, Nanjing 210046, China;
[e] Department of Biochemistry and Molecular Biology, Feist-Weiller Cancer Center, Louisiana State University Health Sciences Center, LA 71130-3932, USA.
[*] Corresponding author:
Yin Lu, Department of Clinical Pharmacy, School of Pharmacy, Jiangsu Key Laboratory for Traditional Chinese Medicine Formulae Research, Nanjing University of Chinese Medicine, 282 Hanzhong Road, Nanjing, Jiangsu, P.R. China, 210029.
Tel: + 86 25 86798154 Fax: +86 25 86798188
E-mail address: luyingreen@126.com (Y. Lu)
Xiang Gao, Model Animal Research Center, Nanjing University, 12 Xuefu Road, Pukou District, Nanjing, Jiangsu, P.R. China, 210061.
Tel: + 86 25 58641598 Fax: +86 25 58641500
E-mail address: gaoxiang@nju.edu.cn (X. Gao)

Summary

Background and Purpose: Cryptotanshinone (CTs) is a major active component of *Salvia miltiorrhiza*, which is often used as Chinese herbal medicine in cancer therapy. Here, we systematically assessed the anti-tumor effect of CTs on two melanoma cell lines with low/high metastatic capacity (B16/B16BL6).

Experimental Approach: MTT and LDH assays were used to evaluate cell growth and cytotoxicity. We assessed the effect of CTs on cell apoptosis or proliferation by Annexin V, TUNEL or BrdU assay. Cell cycle distribution was detected by flow cytometry. The integrity of cell cycle checkpoints was determined by mutational analyses of B-RAF and N-RAS, and the expression of cell cycle associated proteins by western blotting.

Key Results: Treatment with CTs had no obvious effect on cell apoptosis, but significantly inhibited cell proliferation. CTs induced the expression of p53, Chk1 and Chk2 in both B16 and B16BL6. Interestingly, CTs induced G1 arrest in B16BL6 cells, together with an increase in protein levels of p21. By contrast, in B16 cells, CTs induced the G2/M arrest through induction of Cdc25c. Regulation of Cyclin A1, Cyclin B1 and Cdk1/cdc2 expression level might contribute to the different cell cycle patterns in B16 and B16BL6 after CTs treatment.

Conclusions and Implications: CTs could have opposite effects on cell cycle events in melanoma cell lines with different metastatic capacity. This property might offer an opportunity to study the mechanisms underlying the different anti-tumor effects of CTs on B16 and B16BL6.
Key words: cryptotanshinone, cell cycle-arrest, melanoma, B16, B16BL6

Introduction

Melanoma is a cancer that arises from melanocytes, specialized pigmented cells that are found predominantly in the skin [1]. The incidence of melanoma in many countries has risen by 3-8% per year since the mid 1960s [2, 3] and in western populations the number of cases has doubled in the past 20 years [1]. It is an extremely aggressive disease with high metastatic potential and a notoriously high resistance to cytotoxic agents. This is thought to be because melanocytes originate from highly motile cells that have enhanced survival properties [4]. Melanomagenesis is associated with defects in nucleotide excision repair of solar radiation-induced DNA damage, and cell cycle checkpoints that arrest growth after DNA damage and oncogene activation [5].

The identification of new drugs from plants has a long and successful history [6]. *Salvia miltiorrhiza* (Danshen), a well-known traditional Chinese herbal medicine, is widely used in the clinical treatment of different diseases [7-10]. In the Dictionary of Traditional Chinese Medicine Prescription, *Salvia miltiorrhiza* came in fourth place among 1362 anti-cancer classic and empirical prescription by frequency analysis. Chemical constituents of this medicine have been investigated since 1934. Along with more than 20 phenolic acids, about 30 diterpene compounds have been isolated from Danshen, including the relatively abundant tanshinones, such as tanshinone I, tanshinone IIA, cryptotanshinone, dihydrotanshinone [8]. Cryptotanshinone (CTs), as a major active component, has been shown to possess pharmacological activities, such as anti-cholinesterase, anti-inflammatory, anti-oxidative, anti-bacterial, anti-tumor and anti-platelet aggregation properties [11-16]. Recent studies have also shown that CTs is a potential anticancer agent [17, 18]. However, the anti-cancer mechanisms of CTs remains to be elucidated.

Tumorigenesis encompasses multiple processes involving the dysregulation of a number of molecular pathways, such as cell cycle proliferation and apoptosis. The strategy behind some forms of drug therapy is to either retard cell cycle progression or induce apoptosis. The aim of this study was to investigate the possible roles of CTs on melanoma cell lines with different metastatic capacity, including the high-metastatic potential melanoma cell line (B16BL6) and the low-metastatic potential melanoma cell line (B16). The use of pairs of cell lines, one with a very low and the other with a very high capacity to metastasize, offers an opportunity to dissect out the various processes involved.

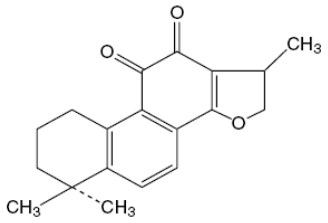

Cryptotanshinone

Materials and methods

Animals

Female C57BL/6 mice (6-8 weeks old) were purchased from the Slac Animal Inc (Shanghai, China). Throughout the experiments, mice were maintained in plastic cages at 21±2 °C, on a 12 h light/dark cycle and with free access to food and water. Animal welfare and experimental procedures were performed strictly in accordance with the care and use of laboratory animals, and the related ethics regulations of our University. All possible efforts were made to minimize the animals' suffering and to reduce the number of animals used.

Cell lines and Culture condition

These studies utilized C57BL/6 mice-derived melanoma cell lines, including B16 (low metastatic potential) and B16BL6 (high metastatic potential). The cells were cultured as a monolayer in DMEM (Gibco, Grand Island, NY, USA), containing 10% v/v Fetal Bovine Serum (Hyclone, Canada), penicillin (100 IU/ml), streptomycin (100 μg/ml) and 3.7 mg/ml $NaHCO_3$. All cells were grown in a humidified atmosphere, containing 5% CO_2 at 37°C.

Experimental metastasis model

The suspension of B16 or B16BL6 cells (5×10^5 cells in 0.2 ml per mouse) were injected through the tail vein of a 6-8 week old female C57BL/6J mice, and allowed to locate to the lungs, where they extravasated into the lung parenchyma. All mice were sacrificed 23 days after the injection of the tumor cells. The lungs were then removed, weighed and fixed. The metastastic foci on the surfaces of the lung were photographed and counted.

MTT assay

In this study, 100 mM stock solution of cryptotanshinone (Xi'an Helin Biological Engineering Co., Ltd. Xi'an, China, purity > 95%) was prepared in ethanol, then filtered by 0.2 μm membrane and diluted as indicated. The growth inhibition effect of cryptotanshinone on melanoma cells was carried out using the MTT assay. Briefly, exponentially growing cells, seeded in 96-well plates (5×10^3 cells/well), were incubated in the presence of different concentrations (0.1 to 100 μM) of cryptotanshinone for different periods of time. At the end of the incubation period 20 μl of a stock solution of 5 mg/ml MTT (Amresco,USA) was added to each well, and plates were gently shaken

and incubated at 37℃. After a further 4 h incubation the cells were lysed with dimethyl sulfoxide and quantified at OD_{490} using an enzyme-linked immunosorbent assay reader.

Cell morphological analysis

Cells were seeded at a density of 1.5×10^5 cells/well in a 6-well plate and grown overnight. The next day, different concentrations of cryptotanshinone were added (final concentration of 0, 1, 10, 25 μM). After incubation for 24 h, images of the cell morphological changes were taken with an inverted microscope at a ×100 magnification by a Leica Qwin system (Leica, LEITZ WETZLAR, Germany).

LDH assay

Cytotoxicity was determined by measuring cell membrane damage through the release of lactate dehydrogenase (LDH), a stable cytosolic enzyme that is released upon cell membrane damage or cell lysis. For this experiment, exponentially growing cells were seeded in 96-well plates (5×10^3 cells/well) and incubated for 24 h in complete medium. The cells were then incubated in the presence of varying concentrations of cryptotanshinone as indicated for 24 h. Culture supernatants were then collected from each well, and the LDH release assay was performed according to the manufacturer's instructions. The LDH kit was purchased from the Nanjing Jiancheng Bioengineering Institute (Nanjing, China).

Anexin V assay

Cells, seeded in 6-well plates at a density of 2×10^5 cells/well in growth medium, were grown overnight at 37°C in a humidified incubator with 5% CO_2. Cells were then treated with cryptotanshinone (0, 1, 10, 25 μM) for 24 h. Cell apoptosis was assessed by Annexin V-FITC staining using a flow cytometric apoptosis detection kit (Cat.No. 556420, BD Biosciences Pharmingen, San Jose, CA). The stained cells with Annexin V-FITC and propidium iodide [7] were analyzed using a BD FACSCalibur™ flow cytometer and CellQuest analysis software (BD Biosciences, Mountain View, CA).

TUNEL assay

Cells (1.8×10^5 cells/well) were seeded in growth medium on Poly-L-Lysine (P4707, Sigma) coated cover glass slides in 6-well plates and grown overnight at 37°C, in a humidified incubator with 5% CO_2. Cells were then treated with cryptotanshinone (0, 1, 10, 25 μM) for 24 h. Then slides were washed with PBS and then fixed in 4% PFA. After rinsing in PBS, cells were examined for apoptosis by terminal deoxynucleotidyl transferase-mediated dUTP nick-end labeling (TUNEL) assay (Promega, Madison, WI) , performed according to the manufacturer's instructions as previously described [19]. Cells were visualized and photographed using Leica TCS-SL confocal system (Leica Microsystems, Mannheim, Germany). At least 5 randomly chosen areas in every slide were used. The TUNEL labelling index was defined as the percentage of TUNEL positive cells against the total number of cells counted.

BrdU assay

Cells (1.8×10^5 cells/well) were seeded in growth medium on Poly-L-Lysine coated

cover glass slides in 6-well plates and grown overnight at 37°C in a humidified incubator, with 5% CO_2. Cells were then treated with cryptotanshinone (0, 1, 10, 25 μM) for 24 h. After that, cells were incubated with BrdU (B5002, Sigma) at a final concentration of 10 μM for 30 minutes at 37℃. The slides were washed with cold PBS prior to fixing with 4% PFA for 10 minutes. Subsequently, slides were washed with PBS and incubated with 2N HCl for 25 minutes. After washing with PBS and incubating with blocking buffer (5% bovine serum albumin, 10% normal goat serum and 0.5% Tween 20 in PBS), the slides were incubated with mouse anti-BrdU antibody (1:100, Roche) at 37℃ for 2 h. The slides were then washed with PBS and incubated with FITC-labeled goat anti-mouse IgG (1:200, Sigma) for 1 hour at room temperature. After washing again, the slides were incubated with Topro-3 (1:300, Invitrogen) in PBS for 15 minutes to counterstain the nuclei, and mounted on slides using 50% glycerol. Cells were visualized and photographed using Leica TCS-SL confocal system. At least 5 randomly chosen areas in every slide were taken. The BrdU labelling index was defined as the percentage of BrdU positive cells against the total number of cells counted.

Cell Cycle assay

Cells were seeded in growth medium in 60-mm dishes at a density of 3×10^5 cells/dish and were grown overnight at 37°C, in a humidified incubator with 5% CO_2. Cells were then treated with cryptotanshinone (0, 1, 10, 25 μM) for 6, 12, 24, 48 h. The population at each stage of the cell cycle was analyzed by flow cytometry. Briefly, cells were trypsinized, washed twice with PBS, and fixed in 70% ethanol over night at -20℃. Fixed cells were then washed with PBS, incubated with 0.5 ml PBS containing 100 μg/ml RNase and stained with 40 μg/ml propidium iodide for 30 min at 37℃. The stained cells were analyzed using a BD FACSCalibur™ flow cytometer and CellQuest analysis software (BD Biosciences, Mountain View, CA).

Mutational Analyses of B-RAF and N-RAS

The N-RAS and B-RAF mutational status was determined from genomic DNA for the melanoma cell lines (B16 and B16BL6). Genomic DNA was isolated from cells, and the mutational status of N-RAS at exons 1 and 2, and B-RAF at exons 14 and 18 were determined as follows: PCR amplification utilized the following primers [20], then PCR products were purified from 1% agarose gels and DNA was sequenced using the forward PCR primers at GenScript Corporation (Nanjing, China)

N-RAS at exon 1 forward: 5'-TTGCTGCTTTTCTACAGG-3',
reverse: 5'-CCAAAGTGAGGATAAGGG-3';
N-RAS at exon 2 forward: 5'-CCTCCTCACTCTTTCATATTCC-3',
reverse: 5'-CAGAAAATATCCCCAGTACC-3';
B-RAF at exon 14 forward: 5'-GGCAGGTCAATATAGTTAGC-3',
reverse: 5'-CGTGTTATACATACCATGTCC-3';
B-RAF at exon 18 forward: 5'-CAAAATGCTTTCTCTAATAGG-3',
reverse: 5'-TAAGCAGTCACTAGTTTAGG-3'.

Western blotting assay

To detect the effects on cell cycle associated protein expression in B16 and B16BL6 cells, cells seeded in 6-well plates at a density of 3×10^5 cells/well in growth medium, were grown overnight at 37°C in a humidified incubator with 5% CO_2. Cells in culture were then treated with different concentrations of cryptotanshinone or media only (control) for 24 h. After that, cells were washed by pre-cooled PBS and lysed in RIPA buffer (50 mM Tris-Cl pH7.4, 150 mM NaCl, 1% NP-40, 0.1% SDS, 0.25% sodium deoxycholate) supplemented with 1 mM PMSF, 1 mM Na_3VO_4, 1 mM NaF, and 1:100 dilution of Protease Inhibitor Cocktail (Sigma, St. Louis, MO, USA). The supernatant containing the protein was collected and the concentration determined by the Bio-Rad Protein Assay (Bio-Rad Laboratories, Inc., Hercules, CA). Protein samples were resolved by SDS-PAGE and transferred to a polyvinylidene difluoride membrane (Millipore, Billerica, MA). p53, Chk1, Chk2, p21, Cyclin A1, Cyclin B1, Cdk1/Cdc2 and Cdc25C proteins were detected by immunoblot with anti-p53 (1:500, NCL-p53-CM5p, NovoCastra, Newcastle, U.K.) , anti-Chk1 (1:200, BS1053, Bioworld Technology, Bioworld, U.S.A.), anti-Chk2 (1:200, BS1391, Bioworld Technology, Bioworld, U.S.A.), anti-p21 (1:200, sc-6246, Santa Cruz Biotechnology, Santa Cruz, CA), anti-Cyclin A1 (1:200, BS1804, Bioworld Technology, Bioworld, U.S.A.), anti-Cyclin B1 (1:200, sc-752, Santa Cruz Biotechnology, Santa Cruz, CA), anti-Cdk1/Cdc2 (1:200, BS1820, Bioworld Technology, Bioworld, U.S.A.), anti-Cdc25C (1:200, sc-327, Santa Cruz Biotechnology, Santa Cruz, CA) polyclonal antibody and β-actin (1:15000; Sigma St Louis, MO, U.S.A.) or GAPDH (1:5000, sc-32233, Santa Cruz Biotechnology, Santa Cruz, CA), then followed by incubation with peroxidase-coupled secondary antibodies. A Supersignal kit (Pierce, Rockford, IL) was used to visualize the bands according to the manufacturer's instructions.

Statistical analysis

The data obtained from at least three independent tests are presented as means±S.E.M and statistical comparisons between groups performed using 1-way ANOVA followed by Student's t-test at P values of <0.001(***), <0.01(**) or<0.05(*).

Results

Effect of CTs on B16 and B16BL6 melanoma cell growth

The aim of this study was to investigate the possible roles of CTs on melanoma cell lines with different metastatic capacity. First of all, we established an *in vivo* experimental metastasis model to confirm the exact metastatic capacity of B16 (low-metastatic potential) and B16BL6 (high-metastatic potential) melanoma cell lines. Compared with the B16 melanoma cell group, B16BL6 melanoma cells increased remarkably the lung weight and the number of tumor nodules on the lung surface in the experimental metastasis model (Supplementary Fig. 1).

We then assessed the effect of CTs on cell growth of B16 and B16BL6 melanoma cell lines *in vitro*. Exponentially growing cells were cultured with different concentrations of CTs for 24 h, and then cell growth evaluated by the MTT assay. As shown in Fig. 1A, CTs caused a strong concentration-dependent inhibition in B16 and B16BL6 melanoma cell growth. IC50 values of CTs on B16 and B16BL6 cells were 12.37 μM and 8.65 μM, respectively. Cells were then treated with various concentrations of CTs (0, 1, 10, and 25 μM) for different periods of time (4, 8, 12, 16, 20 and 24 h) and the MTT assay

performed at the end of each treatment. A marked reduction in viable cell count was observed after treatment with CTs in both a time- and dose-dependent manner (Fig. 1B). At the same time, the cell viability following CTs treatment was further confirmed by morphological analyses. The present results demonstrated that CTs was able to inhibit cell growth and induce morphological changes (Fig. 1C). The cytotoxic effect of CTs on B16 and B16BL6 cells was also determined using the LDH assay (Fig. 1D). We found that cytotoxic effects triggered by CTs occurred at concentrations above 25 μM, with significant effects seen at 50-100 μM, and that there was no significant adverse effect of CTs at lower (0-25 μM) concentrations. These results indicated that the growth inhibition of CTs (0-25 μM) was due to cytostatic rather than cytotoxic effects.

Effect of CTs on B16 and B16BL6 melanoma cell apoptosis

To determine whether the growth inhibitory effect of CTs was associated with the induction of apoptosis, B16 and B16BL6 cells were exposed to CTs (0, 1, 10, and 25 μM) for 24 h. After that, these cells were stained with annexin-V FITC & propidium iodide (PI) and then determined by flow cytometry. As shown in Fig. 2A, CTs increased the percentage of apoptotic cells in a concentration-dependent manner, but the effect was slight. At 25 μM, CTs only induced apoptosis in approximately 4% of Cells. Similar results were obtained in B16BL6 cells, suggesting that the effect of CTs on the induction of apoptosis in both B16 and B16BL6 melanoma cells was of lesser relevance. FITC-linked Annexin V/propidium iodide staining assay provides a simple and effective method to detect apoptosis at a very early stage, while terminal deoxynucleotidyl transferase dUTP nick end labeling (TUNEL) is a method for identifying cells in the last phase of apoptosis. To further strengthen the evidence, TUNEL assay was used to confirm the effect of CTs on apoptosis, and confirmatory results were obtained by TUNEL staining through counting the apoptotic cells (Fig. 2B).

Effect of CTs on B16 and B16BL6 melanoma cell proliferation (DNA Synthesis)

Cell proliferation and apoptosis are intimately linked, thus the coordination, and balance, between these two processes is crucial for normal cell physiology. Although CTs decreased the number of B16 and B16BL6 melanoma cells there was no obvious apoptosis as measured by AnexinV and TUNEL assays. The growth of cells in the presence of BrdU, which is incorporated into newly synthesized DNA of actively proliferating cells, has become an accepted method for monitoring DNA replication [21, 22]. When the cell enters the S phase (DNA Synthesis) the cellular DNA is duplicated, to ensure each daughter cell will receive a complete set of genetic information. To determine the effect of CTs on cell proliferation in the S phase, BrdU incorporation was used to define the kinetics of DNA synthesis after CTs treatment. Cells in S phase were labeled by BrdU incorporation, assayed by immunostaining and counted using Confocal microscopy. CTs treatment resulted in a decreased number of BrdU-positive cells in a dose-dependent manner (Fig. 3), indicating that the percentage of cells in the S phase, and hence undergoing DNA synthesis, was reduced.

Effect of CTs on B16 and B16BL6 melanoma cell cycle

The cell cycle is a critical regulator of the processes involved in cell proliferation and growth, as well as cell division after DNA damage. To explore whether the observed growth inhibitory effect of CTs was caused by specifically perturbing cell cycle-related events, a set of experiments were performed to measure both DNA content and the cell cycle distribution of CTs-treated, or untreated, cells by flow cytometry after staining with PI. As shown in Fig. 4, the population of cells in the S phase continuously decreased both in B16 and B16BL6 cells in a concentration- and time-dependent manner after exposure to CTs, consistent with the results of the BrdU assay. At the same time, the sub-G1 peak (apoptosis peak) was not observable, which was consistent with the results of Anexin V and TUNEL assay. Interestingly, the data indicated that during the 48 h time period, treatment of B16 and B16BL6 cells with CTs led to a marked accumulation of cells in the G2 phase and G1 phase respectively. This effect was both concentration- and time-dependent, suggesting that the growth inhibition was the result of a block during the G1 phase, and that such cells do not enter the S phase. Alternatively, it may suggest that it arises from a block during the G2 phase, and that such cells do not enter the M phase. Such effects were not observed in control cells. The CTs-treated cells (25 μM) showed the typical patterns of DNA content that arrested at G2/M phase in B16 cells (Fig. 4B a) and blocked at G1 phase in B16BL6 cells (Fig. 4B b), respectively.

Mutational Analyses of B-RAF and N-RAS in B16 and B16BL6 cell lines

Defects in DNA damage responses may underlie genetic instability and malignant progression in melanoma. Normal human melanocytes (NHMs) display effective G1 and G2 checkpoint responses to ionizing radiation-induced DNA damage. A majority of melanoma cell lines (11/16) display significant quantitative defects in one or both checkpoints. For example, melanomas with B-RAF mutations as a class display a significant defect in DNA damage G2 checkpoints. In contrast, the epithelial-like subtype of melanomas with wild-type N-RAS and B-RAF alleles display an effective G2 checkpoint, but a significant defect in G1 checkpoint function [5]. In the current experiments, flow cytometry indicated that CTs induced G1 arrest in B16BL6 and G2 arrest in B16. The question was, why did CTs have opposite effects on cell cycle events in these two cell lines? We hypothesized that high-metastatic (B16BL6) and low-metastatic (B16) potential melanoma cell lines could display different defects in cell cycle checkpoint functions, in order for cells to proliferate with the chromosomal instability that characterizes this malignancy. We thus analyzed genomic DNA from B16 and B16BL6 melanoma cell lines for oncogenic mutations in N-RAS and B-RAF. However, sequencing of the PCR products did not reveal any mutations in these two cell lines (data not shown).

Effect of CTs on the expression of cell cycle associated proteins in B16 and B16BL6 melanoma cells

Cell cycle checkpoints are surveillance mechanisms that monitor and coordinate the order and fidelity of cell cycle events. These checkpoints verify whether the processes at each phase of the cell cycle have been accurately completed before progression into the next phase. When defects in the division program of a cell are detected, checkpoints

prevent the pursuant cell cycle transition through regulation of the relevant cyclin-cdk complexes [23]. Cell cycle progression is regulated by checkpoint controls that function to protect the integrity of the genome. Such controls act to prevent cell cycle progression until after completion of prior events [24]. The G1 checkpoint permits repair prior to replication, whereas arrest at the G2 checkpoint permits repair of the genome prior to its mitotic segregation. G1 arrest is controlled primarily by the tumor suppressor p53, which is activated in response to various forms of stress, that binds to the promoters of target genes and induces their transcription [25]. Chk 1 and Chk 2 both function as essential components in the G2 DNA damage checkpoint by phosphorylating Cdc25c in response to DNA damage [26]. We speculated that the different cell cycle events induced by CTs in B16 and B16BL6 cells was correlated with the induction of different checkpoint associated proteins. We thus performed western blotting analysis to assess the levels of cell cycle checkpoint regulators of p53, Chk1 and Chk2. The expression of p53, Chk1 and Chk2 were both increased in B16 and B16BL6 cells at 24 h following treatment with CTs (Fig.5A), though the degree of the increase and the basal expression of p53, Chk1 and Chk2 was slightly different in B16 as compared to B16BL6 cells.

To further understand the molecular mechanisms involved, we next investigated the effects of CTs on the cyclin-dependent kinase (Cdk) inhibitor, p21 [27], which mediates p53-dependent G1 growth arrest. Incubation of B16BL6 cells with CTs, which arrested at G1 phase, caused a dose-dependent increase in p21 protein level. On the other hand, CTs treatment of B16 cells, which led to a cell cycle arrest at G2 phase in these cells, induced only a slight increase in the level of p21 (Fig.5B). In addition, a major and crucial target for Chk1 and Chk2 in cell cycle checkpoints is the dual-specificity phosphatase Cdc25, which dephosphorylates and activates Cdks [28, 29]. We found that the level of Cdc25c was increased in B16, but decreased in B16BL6, cells in response to CTs treatment (Fig.5B).

In mammalian cells, progression through the G2 phase of the cell cycle is mediated by a specific set of proteins, which includes Cyclins A1, B1, mitotic kinase cdk1 (alias p34*Cdc2*) [30]. Western blotting analysis of cell samples obtained after CTs treatment for 24 h showed significant changes in the intracellular protein levels of Cyclin A1, Cyclin B1 and Cdc2 as compared with the untreated control (Fig.5C). After CTs treatment B16 cells in the G2/M phase expressed Cyclin A1,Cyclin B1 and Cdk1/cdc2 at a higher level, while B16BL6 cells in the G1 phase expressed these regulatory proteins at a lower level. Our present study established that CTs induced G1 arrest in B16BL6 cells, together with an increase in p21 protein level. However, CTs blocked B16 cells in G2 phase, along with an accumulation of Cdc25c, Cyclin A1,Cyclin B1 and Cdk1/cdc2 protein level.

Discussion

Melanoma is the second most rapidly growing type of cancer in humans [31]. It is characterized by a high metastatic propensity, resistance to any known cancer therapies, and extremely poor patient survival rate. In this study, the results showed that CTs was a potent inhibitor of B16 and B16BL6 melanoma cell growth. The balance of cell progression is a series of tightly integrated events which allows cells to grow,

proliferate and die. However, we could not detect any obvious apoptosis in CTs-treated cells. Subsequent experiments addressed whether CTs inhibited cell proliferation, as measured by the BrdU assay. The data for CTs-treated cells clearly revealed a significant reduction in cells in the S phase. To confirm that the effect induced by CTs was associated with the arrest of cells in a particular phase, we analyzed cell distribution at each phase of the cell cycle by flow cytometry. We found that CTs inhibited the cell proliferation by inducing the G2/M arrest in a dose-dependent manner in the B16 cell line. This observation was different from the results obtained from the B16BL6 cell line, which showed an increased cell population in the G1 phase.

We hypothesized that CTs induced G1 arrest in B16BL6 cell line (high-metastatic potential) and G2 arrest in B16 cell line (low-metastatic potential), and that this depended on the integrity of different checkpoint controls in these different cell lines, or the different cell cycle regulators induced by CTs. As defects in cell cycle checkpoint function are comparatively common in melanoma cell lines [5], we tested this hypothesis, by investigating whether the two cell lines displayed different defects in cell cycle checkpoint controls by mutational analyses of B-RAF and N-RAS genes. However, sequencing of the PCR products did not reveal any mutations.

We then examined the expression of intracellular proteins involved in regulating the cell cycle at the G1 or G2/M boundary. There are well-known CDK inhibitors, such as $p16^{NK4a}$, $p21^{WAF1/CIP1}$, and $p27^{KIP1}$, which bind to and inhibit the CDK-cyclin complexes [32]. It has been reported that p53 regulates a DNA damage-triggered G1 checkpoint by up-regulation of $p21^{WAF1/CIP1}$ [33]. $p21^{WAF1/CIP1}$ is not only activated by the p53 protein, but it also blocks the cell cycle at the G1 phase [34]. The cell cycle G2/M checkpoint control appears to involve a number of proteins in a wide variety of eukaryotic cells., such as: Cyclin A; Cyclin B; Cdk1/cdc2; Cdc25; Chk1 and Chk2, as well as DNA damage sensor proteins. To explore the molecular mechanisms of CTs-induced cell cycle arrest, we analyzed the levels of these cell cycle regulatory proteins in B16 and B16BL6 cell lines. We demonstrated that CTs induced the expression of p53, Chk1 and Chk2 in both B16 and B16BL6. Interestingly, CTs induced G1 arrest in B16BL6 cells, together with an increase in p21 protein level. By contrast, in B16 cells, CTs induced the G2/M arrest through induction of Cdc25c. Furthermore, regulation of the levels of expression of Cyclin A1, Cyclin B1 and Cdk1/cdc2 might also contribute to the different cell cycle patterns in B16 and B16BL6 cells following CTs treatment. It has been shown that the expression of cell cycle regulatory proteins was activated by CTs, suggesting that CTs-induced G2 arrest in B16 cell line might be mediated via the signaling cascade, involving a distinct cascade of check-point kinases (Chk → Cdc25C → G2 phase). On the other hand, p53 might regulate a DNA damage-triggered G1 checkpoint by up-regulation of $p21^{WAF1/CIP1}$ in CTs-induced B16BL6 cells (p53 → p21 → G1 phase). Thus, we supposed that such phenomenon was correlated to DNA damage and different cell cycle-regulatory proteins status induced by CTs in different metastatic potential melanoma cell lines. These results suggested that modulation of cell cycle-regulatory proteins might be a possible molecular mechanism of the action of CTs.

CTs was shown to arrest B16BL6 cells in G1 and block B16 cells at the G2/M transition. The reason for this difference in behavior induced by CTs in these two cell lines might be due to their distinct properties of these two cell lines. Similar conflicting results have been presented in other reports. For example, quercetin has been shown to block the cell cycle at the G1/S transition in colon and gastric cancer cells as well as in leukemic cells. By contrast, it has been found to cause a G2/M block in breast and laryngeal cancer cell lines, and in non-oncogenic fibroblasts [35]. Similarly, reports have indicated that As_2O_3 treatment resulted in cell-cycle arrest at either G1 or G2/M phase depending on the cell line used [36].

The results also revealed differences in structure-activity relationship between the tanshinones. Mosaddik [37] has studied the cytotoxic effect of four tanshinones isolated from the dried root of *Salvia miltiorrhiza Bunge* on P388 lymphocytic leukemia cells, and suggested that the unsaturation at C-15 and saturation on ring A may be critical structural components for the cytotoxicity of these diterpenes. This result was consistent with our study in that cryptotanshinone, which lacks saturation at C-15, showed little cytotoxicity, but possessed a potent cytostatic effect. Therefore, due to this lack of cytoxic effects, CTs may have potential as a lead compound in the development of chemotherapeutic agents. While the anti-proliferative effect of CTs represent a potential cancer chemopreventive mechanism, the cell cycle effect of CTs *in vivo* also requires further study. Furthermore, CTs, which appears to have opposite effects on cell cycle events in melanoma cell lines with different metastatic capacity, offers a useful tool to investigate the reasons behind such different patterns of malignancy.

Acknowledgements

We are grateful for financial support from National Nature Science Foundation of China (Project No. 30371727, 30772766), Nature Science Foundation of Jiangsu Province (Project No. BK2003113, BK2007239) and Educational Commission of Jiangsu Province (Project No. 09KJA360002). We also appreciate Dr. Bin Chen for the thoughtful revision.

Referrences

1. Gray-Schopfer V, Wellbrock C, Marais R: **Melanoma biology and new targeted therapy.** *Nature* 2007, **445:**851-857.
2. Marquette A, Bagot M, Bensussan A, Dumaz N: **Recent discoveries in the genetics of melanoma and their therapeutic implications.** *Arch Immunol Ther Exp (Warsz)* 2007, **55:**363-372.
3. Lens M: **Current clinical overview of cutaneous melanoma.** *Br J Nurs* 2008, **17:**300-305.
4. Soengas MS, Lowe SW: **Apoptosis and melanoma chemoresistance.** *Oncogene* 2003, **22:**3138-3151.
5. Kaufmann WK, Nevis KR, Qu P, Ibrahim JG, Zhou T, Zhou Y, Simpson DA, Helms-Deaton J, Cordeiro-Stone M, Moore DT, et al: **Defective cell cycle checkpoint functions in melanoma are associated with altered patterns of gene expression.** *J Invest Dermatol* 2008, **128:**175-187.

6. Fan TP, Yeh JC, Leung KW, Yue PY, Wong RN: **Angiogenesis: from plants to blood vessels.** *Trends Pharmacol Sci* 2006, **27:**297-309.
7. Zhang F, Zheng W, Pi R, Mei Z, Bao Y, Gao J, Tang W, Chen S, Liu P: **Cryptotanshinone protects primary rat cortical neurons from glutamate-induced neurotoxicity via the activation of the phosphatidylinositol 3-kinase/Akt signaling pathway.** *Exp Brain Res* 2009, **193:**109-118.
8. Zhou L, Zuo Z, Chow MS: **Danshen: an overview of its chemistry, pharmacology, pharmacokinetics, and clinical use.** *J Clin Pharmacol* 2005, **45:**1345-1359.
9. Wang BE: **Treatment of chronic liver diseases with traditional Chinese medicine.** *J Gastroenterol Hepatol* 2000, **15 Suppl:**E67-70.
10. Yu XY, Lin SG, Chen X, Zhou ZW, Liang J, Duan W, Chowbay B, Wen JY, Chan E, Cao J, et al: **Transport of cryptotanshinone, a major active triterpenoid in Salvia miltiorrhiza Bunge widely used in the treatment of stroke and Alzheimer's disease, across the blood-brain barrier.** *Curr Drug Metab* 2007, **8:**365-378.
11. Hur JM, Shim JS, Jung HJ, Kwon HJ: **Cryptotanshinone but not tanshinone IIA inhibits angiogenesisin vitro.** *Exp Mol Med* 2005, **37:**133-137.
12. Kang BY, Chung SW, Kim SH, Ryu SY, Kim TS: **Inhibition of interleukin-12 and interferon-gamma production in immune cells by tanshinones from Salvia miltiorrhiza.** *Immunopharmacology* 2000, **49:**355-361.
13. Lee DS, Lee SH, Noh JG, Hong SD: **Antibacterial activities of cryptotanshinone and dihydrotanshinone I from a medicinal herb, Salvia miltiorrhiza Bunge.** *Biosci Biotechnol Biochem* 1999, **63:**2236-2239.
14. Ren Y, Houghton PJ, Hider RC, Howes MJ: **Novel diterpenoid acetylcholinesterase inhibitors from Salvia miltiorhiza.** *Planta Med* 2004, **70:**201-204.
15. Ryu SY, Oak MH, Kim KM: **Inhibition of mast cell degranulation by tanshinones from the roots of Salvia miltiorrhiza.** *Planta Med* 1999, **65:**654-655.
16. Wang AM, Sha SH, Lesniak W, Schacht J: **Tanshinone (Salviae miltiorrhizae extract) preparations attenuate aminoglycoside-induced free radical formation in vitro and ototoxicity in vivo.** *Antimicrob Agents Chemother* 2003, **47:**1836-1841.
17. Nizamutdinova IT, Lee GW, Son KH, Jeon SJ, Kang SS, Kim YS, Lee JH, Seo HG, Chang KC, Kim HJ: **Tanshinone I effectively induces apoptosis in estrogen receptor-positive (MCF-7) and estrogen receptor-negative (MDA-MB-231) breast cancer cells.** *Int J Oncol* 2008, **33:**485-491.
18. Shin DS, Kim HN, Shin KD, Yoon YJ, Kim SJ, Han DC, Kwon BM: **Cryptotanshinone inhibits constitutive signal transducer and activator of transcription 3 function through blocking the dimerization in DU145 prostate cancer cells.** *Cancer Res* 2009, **69:**193-202.
19. Zhang W, Li D, Mehta JL: **Role of AIF in human coronary artery endothelial cell apoptosis.** *Am J Physiol Heart Circ Physiol* 2004, **286:**H354-358.
20. Melnikova VO, Bolshakov SV, Walker C, Ananthaswamy HN: **Genomic alterations in spontaneous and carcinogen-induced murine melanoma cell lines.** *Oncogene* 2004, **23:**2347-2356.
21. Gratzner HG: **Monoclonal antibody to 5-bromo- and 5-iododeoxyuridine: A new reagent for detection of DNA replication.** *Science* 1982, **218:**474-475.
22. Dolbeare F, Gratzner H, Pallavicini MG, Gray JW: **Flow cytometric measurement of total DNA content and incorporated bromodeoxyuridine.** *Proc Natl Acad Sci U S A* 1983,

80:5573-5577.

23. Koniaras K, Cuddihy AR, Christopoulos H, Hogg A, O'Connell MJ: **Inhibition of Chk1-dependent G2 DNA damage checkpoint radiosensitizes p53 mutant human cells.** *Oncogene* 2001, **20:**7453-7463.
24. Hartwell LH, Weinert TA: **Checkpoints: controls that ensure the order of cell cycle events.** *Science* 1989, **246:**629-634.
25. Vogelstein B, Lane D, Levine AJ: **Surfing the p53 network.** *Nature* 2000, **408:**307-310.
26. Liu Q, Guntuku S, Cui XS, Matsuoka S, Cortez D, Tamai K, Luo G, Carattini-Rivera S, DeMayo F, Bradley A, et al: **Chk1 is an essential kinase that is regulated by Atr and required for the G(2)/M DNA damage checkpoint.** *Genes Dev* 2000, **14:**1448-1459.
27. Abbas T, Dutta A: **p21 in cancer: intricate networks and multiple activities.** *Nat Rev Cancer* 2009, **9:**400-414.
28. Rhind N, Russell P: **Chk1 and Cds1: linchpins of the DNA damage and replication checkpoint pathways.** *J Cell Sci* 2000, **113 (Pt 22):**3889-3896.
29. Bartek J, Lukas J: **Chk1 and Chk2 kinases in checkpoint control and cancer.** *Cancer Cell* 2003, **3:**421-429.
30. Manni I, Mazzaro G, Gurtner A, Mantovani R, Haugwitz U, Krause K, Engeland K, Sacchi A, Soddu S, Piaggio G: **NF-Y mediates the transcriptional inhibition of the cyclin B1, cyclin B2, and cdc25C promoters upon induced G2 arrest.** *J Biol Chem* 2001, **276:**5570-5576.
31. Rigel DS, Carucci JA: **Malignant melanoma: prevention, early detection, and treatment in the 21st century.** *CA Cancer J Clin* 2000, **50:**215-236; quiz 237-240.
32. Sherr CJ, Roberts JM: **Inhibitors of mammalian G1 cyclin-dependent kinases.** *Genes Dev* 1995, **9:**1149-1163.
33. Hartwell LH, Kastan MB: **Cell cycle control and cancer.** *Science* 1994, **266:**1821-1828.
34. Im EO, Choi YH, Paik KJ, Suh H, Jin Y, Kim KW, Yoo YH, Kim ND: **Novel bile acid derivatives induce apoptosis via a p53-independent pathway in human breast carcinoma cells.** *Cancer Lett* 2001, **163:**83-93.
35. Casagrande F, Darbon JM: **Effects of structurally related flavonoids on cell cycle progression of human melanoma cells: regulation of cyclin-dependent kinases CDK2 and CDK1.** *Biochem Pharmacol* 2001, **61:**1205-1215.
36. Ling YH, Jiang JD, Holland JF, Perez-Soler R: **Arsenic trioxide produces polymerization of microtubules and mitotic arrest before apoptosis in human tumor cell lines.** *Mol Pharmacol* 2002, **62:**529-538.
37. Mosaddik MA: **In vitro cytotoxicity of tanshinones isolated from Salvia miltiorrhiza Bunge against P388 lymphocytic leukemia cells.** *Phytomedicine* 2003, **10:**682-685.

Figures and Figure legends

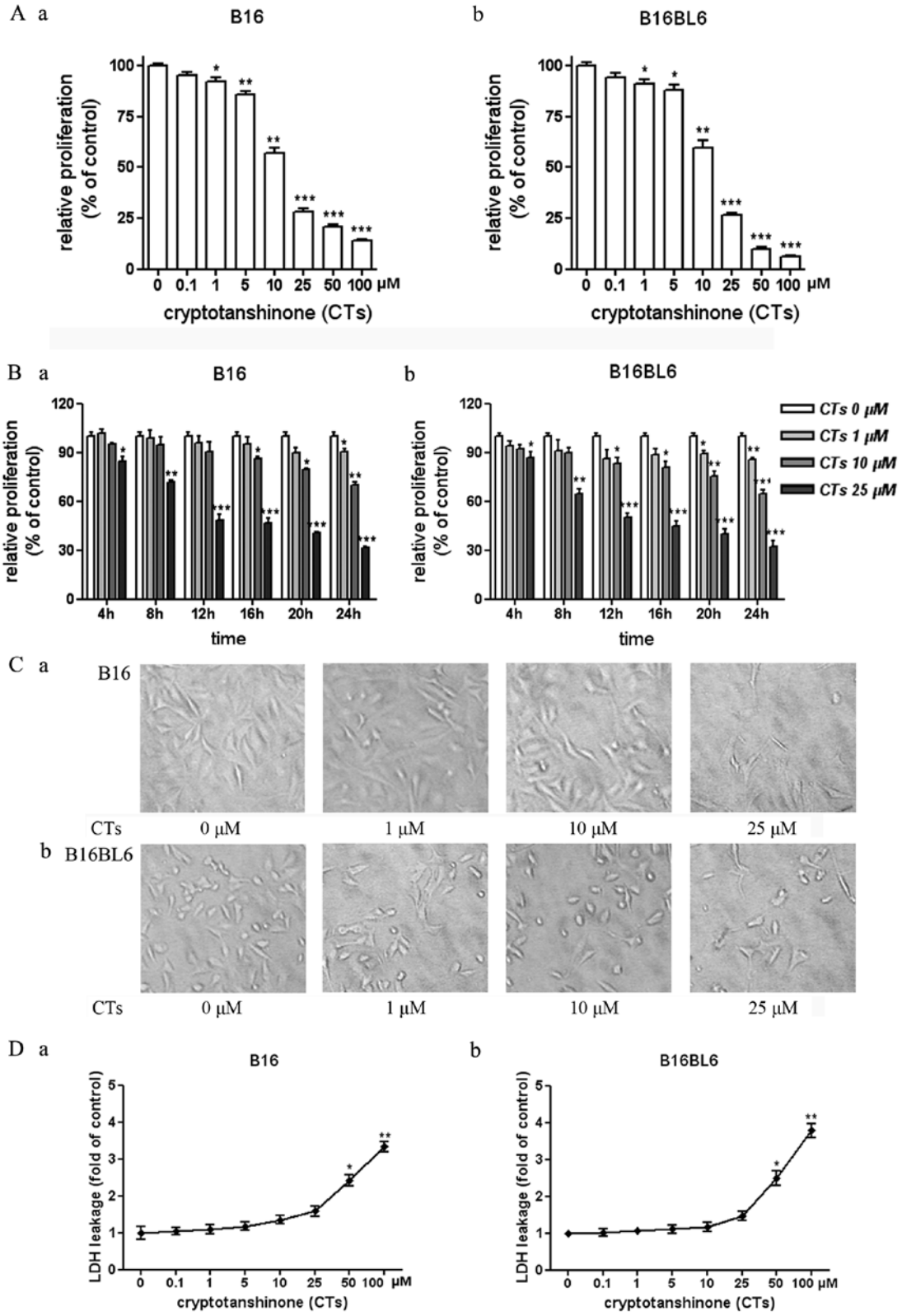

Fig.1. Effect of CTs on B16 and B16BL6 melanoma cell growth. **(A)** The effect of CTs in different concentrations on B16 and B16BL6 melanoma cell growth. **(B)** The effect of CTs on B16 and B16BL6 melanoma cell growth at different time points. The cell growth was evaluated by MTT assay. The reading of control was normalized to 100%, and readings from CTs-treated cells were

expressed as % of control (CTs 0 μM). **(C)** The effect of CTs on B16 and B16BL6 melanoma cell morphology. After incubation with CTs for 24 h, images of the cell morphological changes were taken with an inverted microscope at a ×100 magnification. **(D)** The cytotoxic effect of CTs on B16 and B16BL6 melanoma cell. After treatment with CTs for 24 h, culture supernatants were then collected and cell cytotoxicity was measured by LDH release assay. Values are presented as fold normalized activity relative to that of control. Data are all presented as mean±s.e.m (*= P <0.05, **= P< 0.01, ***= P< 0.001 versus control). **(a)** for B16 melanoma cell line; **(b)** for B16BL6 melanoma cell line.

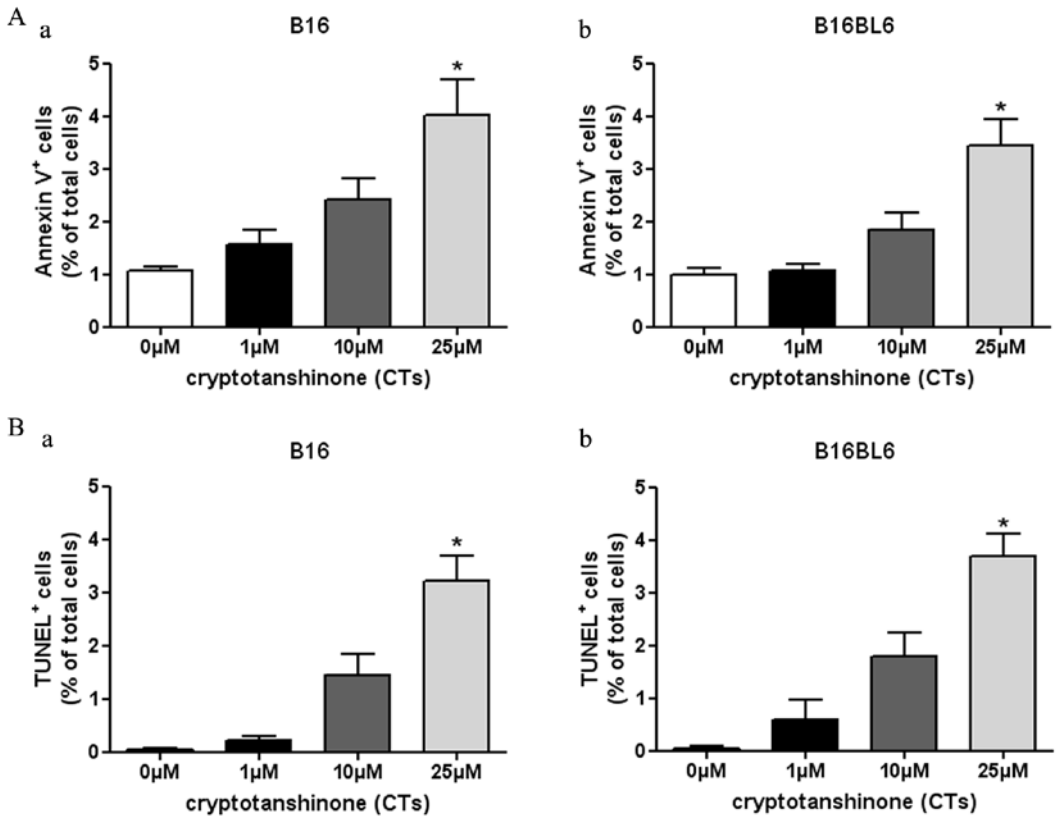

Fig.2. Effect of CTs on B16 and B16BL6 melanoma cell apoptosis. **(A)** The effect of CTs on B16 and B16BL6 melanoma cell apoptosis in the early stage. **(B)** The effect of CTs on B16 and B16BL6 melanoma cell apoptosis in the last phase. Proliferating cells were exposed to CTs (0, 1, 10, and 25 μM) for 24 h, and the apoptotic cells in the early stage were determined by Annexin V/PI using flow cytometric analysis. The Annexin V labelling index was defined as the percentage of Annexin V positive and PI negative cells against total cells counted. The apoptotic cells in the last phase were measured by TUNEL immunofluorescence assay, then visualized and photographed using Leica TCS-SL confocal system. At least 5 randomly chosen areas in every slide were taken. The TUNEL labelling index was defined as the percentage of TUNEL positive cells against total cells counted. Columns, mean of triplicates; bars, ±s.e.m (*= P <0.05 versus control). **(a)** for B16 melanoma cell line; **(b)** for B16BL6 melanoma cell line.

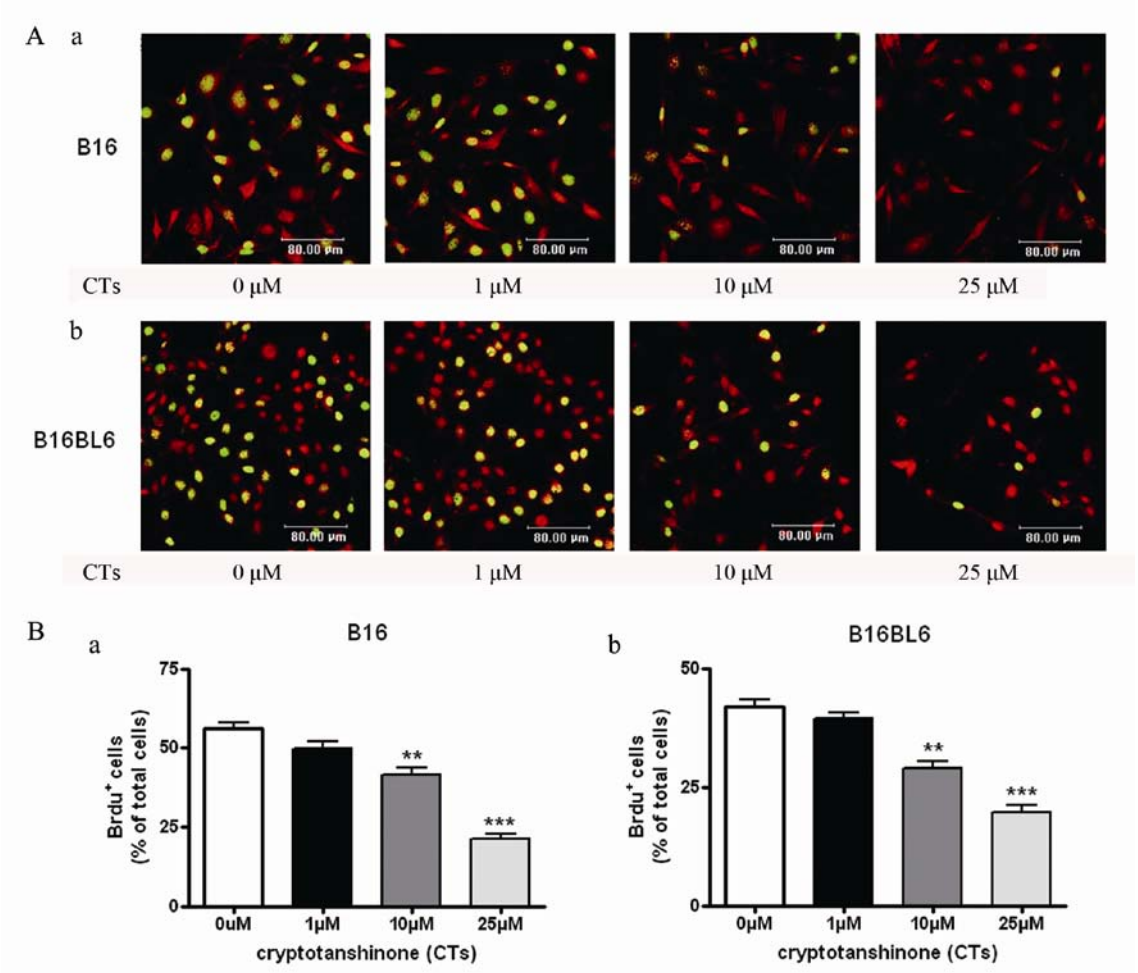

Fig.3. Effect of CTs on B16 and B16BL6 melanoma cell proliferation (DNA Synthesis). Cells were seeded on Poly-L-Lysine coated cover glass slides in 6-well plates, and treated with CTs (0, 1, 10, 25μM) for 24 h. After that, cells were incubated with BrdU at a final concentration of 10 μM for 30 minutes. Cells in S phase (DNA Synthesis) were labelled by BrdU incorporation, assayed by immunostaining and counted by confocal microscope. The representative photographs of immunofluorescence of BrdU (green) and Topro-3 (red) in CTs treated cells were shown in **(A)**. At least 5 randomly chosen areas in every slide were taken. The BrdU labelling index was shown in **(B)**, which defined as the percentage of BrdU positive cells (green) against total cells (red) counted. Columns, mean of triplicates; bars, ±s.e.m (**= P <0.01, ***= P <0.001 versus control). **(a)** for B16 melanoma cell line; **(b)** for B16BL6 melanoma cell line.

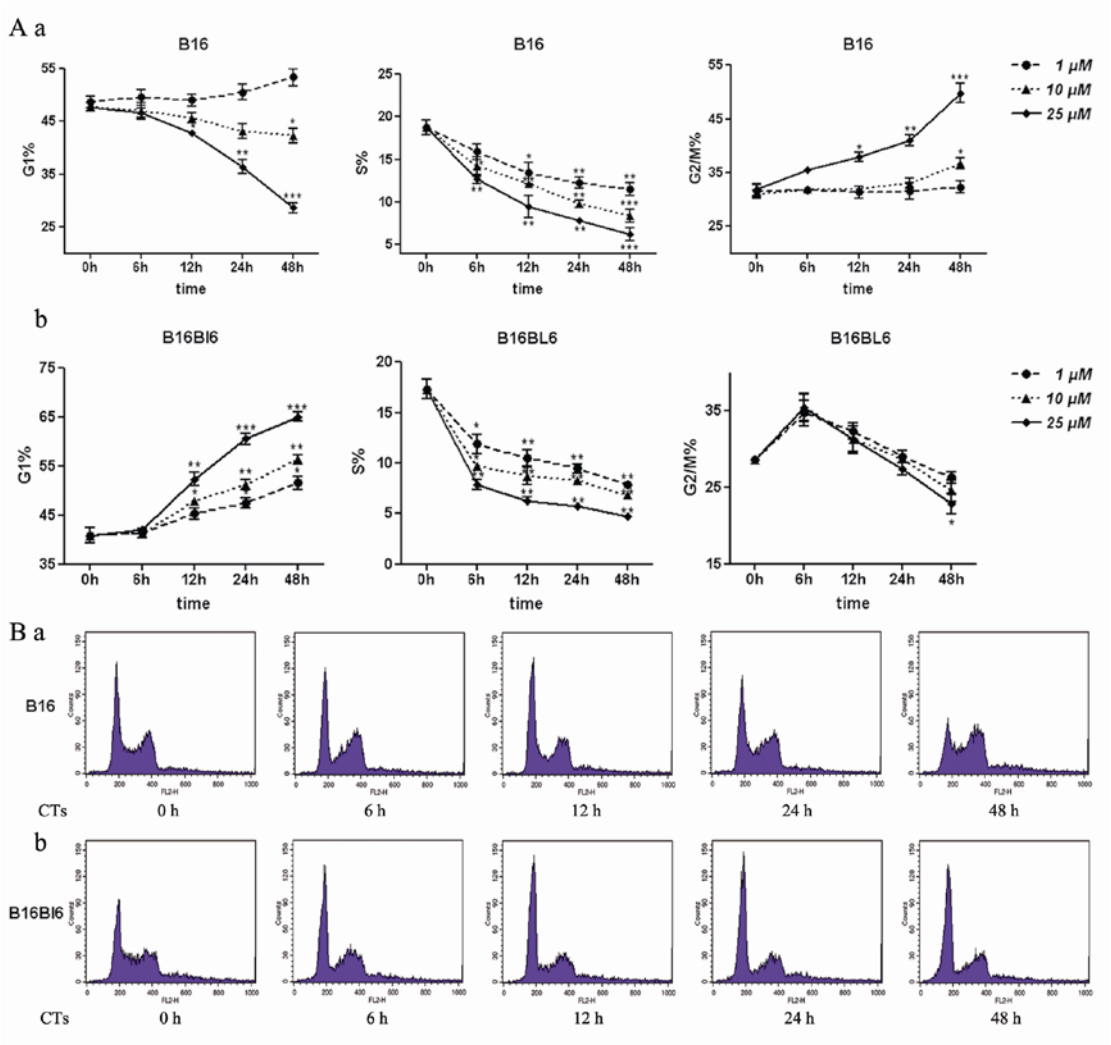

Fig.4. Effect of CTs on B16 and B16BL6 melanoma cell cycle. Cells were plated at $3x10^5$ cells per 60-mm dish, incubated for 12 h, transfered to fresh medium and treated with different concentrations of CTs (0, 1, 10, 25 μM) for 0, 6, 12, 24,48 h. After incubation for different periods of time, cells were collected, stained and analyzed by flow cytometry for cell distribution at each phase of the cell cycle. **(A)** Calculation of cell cycle distribution using CellQuest analysis software. Data are the means ±s.e.m obtained from a triplicate of each experiment. *= P <0.1, **= P <0.01, ***= P <0.001 versus control (CTs 0 μM, 0 h). **(B)** The typical pattern of DNA content of cell cycle distribution in CTs (25 μM) treated cells at different time points. **(a)** for B16 melanoma cell line; **(b)** for B16BL6 melanoma cell line.

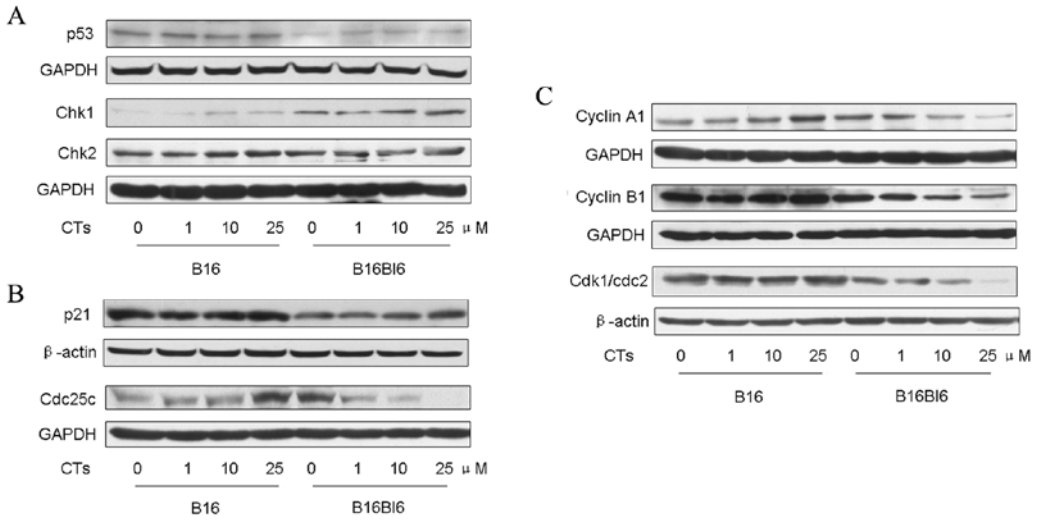

Fig.5. Effect of CTs on the expression of cell cycle associated proteins in B16 and B16BL6 melanoma cells. Cells were treated with CTs (0, 1, 10, 25 μM) for 24 h. Whole cell extracts were analyzed by western blotting using the indicated antibody. β-actin or GAPDH was used as an internal control to monitor equal protein loading. **(A)** The effect of CTs on the expression of p53, Chk1 and Chk2 in B16 and B16BL6 melanoma cells. **(B)** The effect of CTs on the expression of p21 and Cdc25c in B16 and B16BL6 melanoma cells. **(C)** The effect of CTs on the expression of Cyclin A1, Cyclin B1 and Cdk1/cdc2 in B16 and B16BL6 melanoma cells.

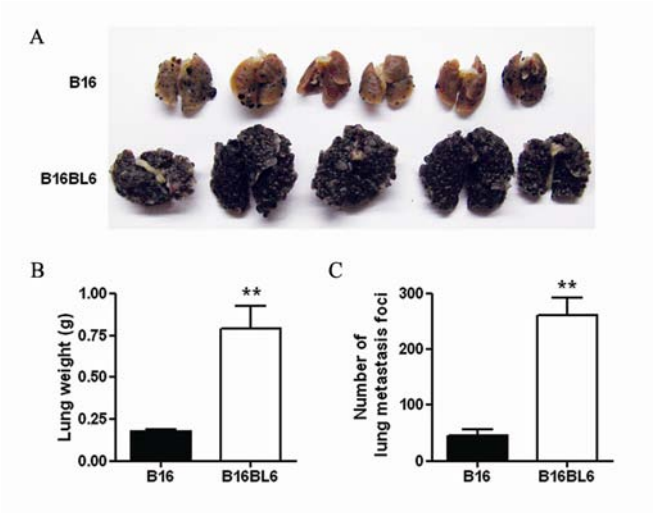

Supplementary Fig.1. Comparison of metastatic behavior between B16 and B16BL6 melanoma cells. In a model of experimental metastasis, mice were sacrificed at 23 days after tumor cells injection. The lungs were removed, washed with PBS, and fixed in 10% v/v formaldehyde. The metastatic colonies were counted under a dissecting microscope. **(A)** The lungs were photographed to show the capacity of metastasis between B16 and B16BL6 melanoma cells. **(B)** The lung weight of B16 and B16BL6 group in experimental metastasis model. **(C)** The number of lung metastasis foci in each group. Columns, mean: B16 group (n=6), B16BL6 group (n=5); bars, ±s.e.m., ** = P< 0.01 versus B16 group.